Chitosan Fiber as Green Material for Removing Cr(VI) and Cu(II) Contaminants:Adsorption Properties,Kinetics and Machanism

shujie Zhang (1512238931@qq.com)
Tiangong University
Yating Zhang
Tiangong University
Lisong Fu
Tiangong University
Mengke Jing
Tiangong University

Research Article

Keywords: Chitosan fiber, Adsorption mechaniam, Adsorption kinetics, contaminated water, Cr(VI) and Cu(II) removal

Posted Date: August 3rd, 2021

DOI: https://doi.org/10.21203/rs.3.rs-754383/v1

Abstract

Chitosan (CS) fiber is used as a new green material to remove Cu(II) and Cr(VI) in wastewater.Varying factors, including pH value, dosage of CS, reaction time and original Cr (VI) contents and Cu(II) were studied to investigate the Cr (VI) and Cu(II) removal efficiency.The adsorption of two metal ions by chitosan fiber conforms to the second-order kinetic equation, and can be fitted with Langmuir isotherms. The adsorption process is a spontaneous thermal reaction with both physical adsorption and chemical adsorption, and copper ions reach adsorption equilibrium. It takes longer than chromium ions, but the adsorption effect of copper ions is better. The maximum actual adsorption capacity of copper ions is 539.6 mg/g, and the maximum adsorption capacity of chromium ions is 75 mg/g. SEM, FTIR and XRD were used to characterize the physicochemical properties of CS fiber. The result shows that the complex process of the Cr (VI) and Cu(II) removal involves physical and chemical adsorption, CS fiber have exerted significant role in Cr (VI) and Cu(II) removal.

1. Introduction

With the rapid development of industrial economy, heavy metals such as copper and chromium contained in industrial wastewater will cause serious environmental pollution[1-5]. Heavy metals can cause serious harm to the human body, such as chromium: it can cause numbness of the limbs and mental disorders, and copper can cause arthritis and accelerate human aging[6-10]. The concept of "cleaner production" was put forward in the 1950s and 1960s. The concept was to quickly realize the impact of industrial development on the environment, thereby establishing a safe and friendly environmental concept. Now that the concept of environmental protection has been deeply rooted in the hearts of the people, economic development is gradually pursuing green[11-17].

At present, many treatment methods are applied to remove heavy metals, includingg membrane separation, chemical precipitation, solvent extraction, ion-exchange, reduction, reverse osmosis and adsorption[1,18], The adsorption method is widely used for its good results with the advantages of non-production of potential secondary pollutants, recyclable usage, easy accessibility and high efficient usage.

Chitosan is widely used in the fields of food, medicine and wastewater due to its excellent biocompatibility, biodegradability, non-toxicity, adsorption and antibacterial properties. Nowadays, In the study of the adsorption of heavy metal ions, chitosan derivatives have excellent performance except relatively expensive price. Chitosan fiber(CS) is dissolved in acid solution, the used CS can be re-dissolved and produced to achieve recycling, meeting the requirements of sustainable development and saving resources. At present,there are few studies on the use of CS for heavy metal adsorption.

In the previous research on the removal of heavy metal ions in wastewater, chitosan and modified substances were mostly used as adsorbents, and the research and application of chitosan fibers were very few. In this paper, chitosan fiber is used as the experimental material to discuss the influence of

chitosan fiber, metal chromium ion and copper ion on reaction time, copper ion concentration, temperature and pH value. The kinetic and thermodynamic analysis of the adsorption process were carried out, and the adsorption mechanism was characterized by SEM, FTIR and XRD. It is expected to provide a basis for the application and expansion of chitosan fiber in water treatment fields such as water purification or sewage treatment.

2. Materials And Instruments

Materials: The CS was purchased from Tianjin Zhongsheng Co.,LTD.(china). The average length of CS is 40mm, and the linear density is 1.3D.

Copper sulfate pentahydrate, potassium chromate, mmonia water, Ethyi Alcohol(Aladdin Reagent Co., Ltd.), Escherichia coli, Staphylococcus aureus(Nanjing Lezhen Biotechnology Co.,Ltd.), Filter tube(Kunshan Huangda Plastic Products Co., Ltd.).

Instruments:UV spectrophotometer (model is SPECORD®210PLUS), The emission scanning electron microscope (SEM, TM330), The marμX2G X-ray diffractometer was used in X-Ray Diffraction (XRD).

3. Experiments Methods And Fitted Models

3.1 Experimental test methods

Performance test of the CS to remove Cr (VI) and Cu(II) was conducted within a flask with 250 mL capacity. The employed Cr (VI) and Cu(II) solution quantity was 100 mL in each experiment. The 0.1 mol/L HCL and NaOH were utilized for adjusting solution pH value. The speed and temperature of shaker kept at 90 rpm and 288 K, respectively. After reaction, the filtrate is collected for analyzing Cr (VI) and Cu(II) concentration. The experimental methods of Cr(VI) are presented in Table 1.

Table.1

Experimental methods in this study.

set	Experiment factors	pH value	CS content(g)	Reaction time(min)	Original content(mg/L)
1	Effect of pH value	1/3/5/7 9/11/13	0.05	90	100
2	Effect of CS dosage	7	0.025/0.050/0.075/ 0.1/0.125/0.15	90	100
3	Effect of reaction time	7	0.05	5-180	100
4	Effect of initial concentration	7	0.05	90	50/75/100 125/150
5	Adsorption kinetic	7	0.05	5-180	50/100/150
6	Adsorption isotherm	7	0.05	90	50/75/100 125/150

3.2 Determination of Cr (Ⅵ) and Cu(II) concentration

The adsorption capacity and adsorption efficiency of the fiber to Cr(VI) and Cu(II) are calculated by formulas (1), (2) and (3) respectively.

$$q_t = \frac{V(C_0 - C_t)}{1000 \times M} \quad (1)$$

$$q_e = \frac{V(C_0 - C_e)}{1000 \times M} \quad (2)$$

$$E_t = \frac{(C_0 - C_t)}{C_0} \times 100\% \quad (3)$$

In the formula: C_0 represents the original Cr (VI) and Cu(II) content (mg/L), while C_e represents Cr (VI) and Cu(II) content (mg/L) at time e, C_t represents Cr (VI) and Cu(II) content (mg/L) at time t, V represents Solution volume (mL), M represents dry weight of fiber (g).

4. Results And Discussion

4.1 Effect of single factor on Cr (VI) and Cu(II) removal

It can be seen from Figure 1 (a) that as the reaction time increases, the amount of adsorption of Cr(VI) by the fiber increases, and the adsorption rate is faster in the first 60 minutes. It can be clearly seen that the adsorption capacity reaches the maximum at 180 minutes, and the adsorption capacity tends to balance at 180 minutes.50mg/L 100mg/L and 150mg/L Cr(VI) solutions with different concentrations show the same adsorption tendency.

It can be seen from Figure 1(b) that as the pH value of the Cr(VI) solution increases, the adsorption capacity of the fiber to Cr(VI) increases first, and the adsorption capacity of the fiber is the largest when the pH is 3, so the pH value is 3 Determined as the best adsorption pH value of Cr(VI) solution. When the pH of the solution is higher than 7, the absorption of Cr(VI) by the fiber begins to decrease.

It can be seen from Figure 1(c) that as the temperature increases, the amount of adsorption of Cr(VI) by the fiber increases. The adsorption capacity slowed down after 35℃, and the adsorption capacity showed a constant trend at 55℃. 35℃can be determined as the best adsorption temperature, and heating is beneficial to the adsorption of fibers.

Figure 1(d) shows the experimental effect of the amount of chitosan fiber on the removal of Cr (VI). The figure shows that the removal rate increases as the amount of chitosan fiber increases. This is mainly because as the amount of chitosan fiber increases, the number of effective active sites that can react with Cr (VI) increases, so that there is more mutual reaction between chitosan fiber and Cr (VI).

The experiment on the effect of Cr (VI) concentration on Cr (VI) removal efficiency was explored. The results are shown in Figure 1(e). It can be clearly seen that the Cr (VI) removal efficiency decreases with the increase of Cr (VI) concentration. After the action time of chitosan fiber and Cr(VI) is 180 min, when the initial concentration of Cr(VI) is 25mg/L, the best removal rate is 42.8%. The experimental results can show that CS fiber is more suitable for reaction with low concentration of Cr(VI).

Fig.2 Indicates the adsorption performance of CS fiber on Cu(II) shows the same trend as that on Cr(VI), but the adsorption performance on Cu(II) is better. As CS fiber dosage is 0.05g, after 180min reaction, the optimal removal rate 98.7% was obtained with the initial concentration of Cu(II) at 200mg/L. It might be the functional group amino of CS fiber has better adsorption property for divalent metal ions.

4.2 Kinetic experiments

As showed in Fig.3 and Tab.2. According to the value of R^2, $R_2{}^2$>$R_1{}^2$,it can be concluded that the adsorption of Cr(VI) is more in line with the second-order kinetics. Hence, pseudo-second-order kinetic equations are suitable for explaining adsorption profiles. The kinetic parameter R^2 is less than 1, which indicates the favor adsorption profile.

It can see from Fig.4 and Tab.3, the kinetic equation of the CS fiber for the adsorption of Cu(II) has the same properties as that of Cr(VI). the kinetic simulation using pseudo-first-order is not good and the

actual data deviates seriously from the fitted curve. At the same time, the correlation coefficient of kinetic parameters is low. While the pseudo-second-order kinetic plot, with high correlation coefficient of kinetic parameters.

Table 2.

Kinetic model parameters of Cr(VI)

C□mg/L)	Quasi-first order kinetic equation		Quasi-second-order kinetic equation	
set	Linear regression equation	R_1^2	Linear regression equation	R_2^2
50	y=-0.0235*X+2.0467	0.9713	y=0.0373*X+0.1869	0.9974
100	y=-0.0429*X+3.7166	0.9344	y=0.0187*X+0.0409	0.9991
150	y=-0.0341*X+2.7682	0.9833	y=0.0127*X+0.0593	0.9988

Table 3

Kinetic model parameters of Cu(II)

C□mg/L)	Quasi-first order kinetic equation		Quasi-second-order kinetic equation	
	Linear regression equation	R_1^2	Linear regression equation	R_2^2
200	y=-0.09322*X+149.84	0.9662	y=0.0028*X+0.0217	0.9899
300	y=-1.2226*X+210.7589	0.9434	y=0.0019*X+0.0158	0.9877

4.3 Isotherm experiments

From the parameters $R_1^2<R_2^2$ in Figure 5 and Table 4, we can see that the adsorption of Cr(VI) by chitosan fibers is more in line with the Langmuir model, and the adsorption process is multi-layer adsorption. At a temperature of 288K, the maximum theoretical saturated adsorption capacity of chitosan fiber for Cr(VI) is 111mg/g. Since 0<RL<1, the adsorption process is favorable. According to Freundlieh model, parameter 1/n value is between 0 and 1, indicating that the experimental concentration range is beneficial for Cr (VI) adsorption onto CS fiber.

In addition, based on the analysis of Cr(VI), we can get Freundlich model was used to illustrate non-ideal adsorption for the non-uniform surfaces and multilayer adsorption. We can see from Fig.6 and table5. A high k_f value indicates the high affinity of CS fiber for Cu (II) ions.

Table 4

Fitting parameters of adsorption isotherms of Cr(VI)

Langmuir					Freundlich		
Q_e/mg/g	Q_m/mg/g	K_L	R_L	R_1^2	K_f	1/n	R_2^2
75	111	0.014	0.742	0.6062	15.5	0.863	0.9923

Table 5

Fitting parameters of adsorption isotherms of Cu(II)

Langmuir					Freundlich		
Q_e/mg.g^{-1}	Q_m/mg.g^{-1}	K_L	R_L	R_1^2	K_f	1/n	R_2^2
539.6	588.24	0.196	0.048	0.9966	195	0.315	0.8815

4.4 Adsorption mechanism

4.4.1SEM analysis

Fig.7(a) shows the surface of the CS material before adsorption is relatively smooth, Compare the surface of the material after adsorption of chromium(Fig.7(b)) and copper(Fig.7(c)), and the surface of the CS material after adsorption is rough, which is conducive to the adsorption of copper and chromium ions in the next step, Compare the surface of the material after adsorption of copper and chromium, the surface of the CS material after adorption with Cu(II) is more rough. A large amount of copper ions are uniformly distributed on the adsorbed material, which shows that the CS material has high adsorption.

4.4.2 XRD results

AS show in Fig.8. CS fiber has two different crystal forms, both of which belong to the monoclinic crystal system, namely Form I (2θ in10˚) and Form (2θ is about 20˚). As can be seen from Figure 5, CS fiber has a broad crystallization peak at 2θ=10.9˚, which represents the hydrated crystals of chitosan. It is due to the fact that water molecules enter the chitosan. After reacting with chromium, the peak at about 10˚ disappears, It shows that after the adsorption of CS molecules with chromium, the separation is weakened.The regularity of the three-dimensional structure of the sub-chain reduces the intramolecular crystalline area.

In addition, After contact with copper ions, the peak at about 20˚ disappears.This also indicates that the functional groups of chitosan fibers have chelated and cross-linked with copper ions.

4.4.3 FTIR pattern

Fig.9 shows that the infrared spectra of chitosan fiber before and after the absorption of copper ions are roughly similar, and the position of the characteristic absorption peak is based on the original value remains unchanged, the chitosan fiber is more polar than the copper ion after adsorption. This is because after the -OH in the chitosan fiber forms a coordination bond with Cu(II), it breaks the hydrogen bond between -OH, and then The added Cu(II). steric hindrance effect indicates that Cu(II) has been complexed with chitosan fiber. Chromium ions show the same trend.

5. Conclusion

Chitosan fiber adsorbs Cu(II), and the adsorption process conforms to the second-order kinetic equation, and electrochemical adsorption plays a leading role. The adsorption isotherm is more in line with the Langmuir model, and the adsorption process is multi-layer adsorption, which belongs to the spontaneous thermal reaction with both physical adsorption and chemical adsorption, and the adsorption type is effective adsorption. The optimal adsorption reaction time is 90 minutes, the equilibrium adsorption time is 180 minutes, the optimal adsorption pH is 5, and the maximum saturated adsorption capacity can reach 248.4 mg/g. The adsorption of chromium ions and copper ions by chitosan fibers shows the same trend, and the adsorption of low-valent ions by chitosan fibers is better due to cross-linking.

According to the test results of SEM, it can be concluded that the surface of chitosan fiber adsorbs copper ions and becomes rougher. According to the results of FTIR and XRD, it can be obtained that chitosan fiber adsorbs heavy metal ions, mainly physical and chemical adsorption.

Chitosan fiber can be dissolved in acetic acid, and the spinning solution of chitosan fiber is under acidic conditions, which is beneficial to recovery. Spinning into chitosan yarn or other textiles, used in water purification and other water treatment fields, can remove harmful metal ions. It is an environmentally friendly material that can be recycled continuously and has broad application and development prospects.

Declarations

Acknowledgements

This research was financially supported by the National Youth Foundation of China (51303128) and the Natural Science Foundation of Tianjin (15JCZDJC38400).

References

1. Liuyang, X. Y., Yang, H., Huang, S. Y., Zhang, Y. & Xia, S. B. Resource utilization of secondary pyrolysis oil-based drilling cuttings ash for removing Cr (VI) contaminants: Adsorption properties, kinetics and mechanism.J ENVIRON CHEM ENG8,9(2020).
2. Alayu, E. & Leta, S. Post treatment of anaerobically treated brewery effluent using pilot scale horizontal subsurface flow constructed wetland system. *Bioresources and Bioprocessing*, **8**, 19 (2021).
3. Shu, J. C. *et al.* Enhanced removal of Mn2+ and NH4+-N in electrolytic manganese metal residue using washing and electrolytic oxidation. *SEP PURIF TECHNOL*, **270**, 8 (2021).
4. Lu, S. H. *et al.* Insight the roles of loosely-bound and tightly-bound extracellular polymeric substances on Cu^{2+}, Zn^{2+} and Pb^{2+} biosorption process with Desulfovibrio vulgaris.J COLLOID INTERF SCI. 596,408–419.
5. Zhang, T. H., Li, P. Y., Ding, S. P. & Wang, X. F. High permeability composite nanofiltration membrane assisted by introducing TpPa covalent organic frameworks interlayer with nanorods for desalination and NaCl/dye separation. *SEP PURIF TECHNOL*, **270**, 11 (2021).
6. Sasmaz, A., Dogan, I. M. & Sasmaz, M. Removal of Cr, Ni and Co in the water of chromium mining areas by using Lemna gibba L. and Lemna minor L. *WATER ENVIRON J*, **30**, 235 (2016).
7. Lopez-Vinent, N., Cruz-Alcalde, A., Gimenez, J., Esplugas, S. & Sans, C. Improvement of the photo-Fenton process at natural condition of pH using organic fertilizers mixtures: Potential application to agricultural reuse of wastewater. *APPL CATAL B-ENVIRON*, **290**, 11 (2021).
8. Wang, D., Ha, M. M. & Qiao, J. F. Data-Driven Iterative Adaptive Critic Control Toward an Urban Wastewater Treatment Plant.IEEE T IND ELECTRON,68(8),7362–7369.
9. De Lille, M. I. V., Cardona, M. A. H., Xicum, Y. A. T. & Giacoman-Vallejos, G. and C. A. Quintal-Franco,Hybrid constructed wetlands system for domestic wastewater treatment under tropical climate: Effect of recirculation strategies on nitrogen removal. *ECOL ENG*, **166**, 11 (2021).
10. Zhang, H. W. *et al.* and J. Y. Ma,Partial oxidation of phenolic wastewater using NaOH and Ni addition for hydrogen production and phenolics degradation in supercritical water. *SEP PURIF TECHNOL*, **268**, 10 (2021).
11. Liu, X. S., Su, X. M., Tian, S. J., Li, Y. & Yuan, R. F. Mechanisms for simultaneous ozonation of sulfamethoxazole and natural organic matters in secondary effluent from sewage treatment plant. *FRONT ENV SCI ENG*, **15**, 12 (2021).
12. Jiang, X., Pan, W. Y., Xiong, Z. L., Zhang, Y. X. & Zhao, L. S. Facile synthesis of layer-by-layer decorated graphene oxide based magnetic nanocomposites for beta-agonists/dyes adsorption removal and bacterial inactivation in wastewater. *J ALLOY COMPD*, **870**, 12 (2021).
13. Wang, K. *et al.* Earth-abundant metal-free carbon-based electrocatalysts for Zn-air batteries to power electrochemical generation of H2O2 for in-situ wastewater treatment. *CHEM ENG J*, **416**, 8 (2021).
14. Pan, J. W. *et al.* and Q. Y. Yue, n-situ Cu-doped carbon-supported catalysts applied for high-salinity polycarbonate plant wastewater treatment and a coupling application.CHEM. *ENG J*, **416**, 11 (2021).

15. Maifadi, S., Mhlanga, S. D., Nxumalo, E. N., Motsa, M. M. & Kuvarega, A. T. Carbon nanotube embedded ultrafiltration membranes for the treatment of rapid granular multimedia prefiltered beauty hair salon and municipal wastewater.SEP PURIF TECHNOL, 267,15(2021).
16. Virga, E., Parra, M. A. & de Vos, W. M. Fouling of polyelectrolyte multilayer based nanofiltration membranes during produced water treatment:The role of surfactant size and chemistry. *J COLLOID INTERF SCI*, **594**, 9 (2021).
17. Chai, Y. Z. *et al.* A coupled system of flow-through electro-Fenton and electrosorption processes for the efficient treatment of high-salinity organic wastewater. *SSEP PURIF TECHNOL*, **267**, 13 (2021).
18. Gaydukova, A. & Kolesnikov, V. and H. T. Aung,Electroflotosorption method for removing organic and inorganic impurities from wastewater. *SEP PURIF TECHNOL*, **267**, 5 (2021).
19. Teng, X. L. *et al. Effective degradation of atrazine in wastewater by three-dimensional electrochemical system using fly ash-red mud particle electrode: Mechanism and pathway* 26712(SEP PURIF TECHNOL, 2021).
20. Almansba, A. *et al.* Innovative photocatalytic luminous textiles optimized towards water treatment: Performance evaluation of photoreactors. *CHEM ENG J*, **416**, 13 (2021).
21. Medina-Rodriguez, D. F. *et al.* Removal of Pb(II) in Aqueous Solutions Using Synthesized Zeolite X from Ecuadorian Clay. *REV ING INVES*, **41**, 12 (2021).
22. de Oca-Palma, R. M., Solache-Rios, M., Jimenez-Reyes, M. & Garcia-Sanchez, J. J. and P. T. Almazan-Sanchez,Adsorption of cobalt by using inorganic components of sediment samples from water bodies. *INT J SEDIMENT RES*, **36**, 524 (2021).
23. Moneer, A. A., El-Mallah, N. M., El-Sadaawy, M. M., Khedawy, M. & Ramadan, M. S. H. Kinetics, thermodynamics, isotherm modeling for removal of reactive Red 35 and disperse yellow 56 dyes using batch bi-polar aluminum electrocoagulation. *ALEX ENG J*, **60**, 4139 (2021).
24. Babazadeh, M., Abolghasemi, H., Esmaeili, M., Ehsani, A. & Badiei, A. Comprehensive batch and continuous methyl orange removal studies using surfactant modified chitosan-clinoptilolite composite. *SEP PURIF TECHNOL*, **267**, 19 (2021).
25. Foroutan, R., .Peighambardoust, S. J. & Hosseini, S. S. A.Akbari, and B. Hydroxyapatite biomaterial production from chicken (femur and beak) and fishbone waste through a chemical less method for Cd2+ removal from shipbuilding wastewater. *J HAZARD MATER*, **413**, 13 (2021).

Figures

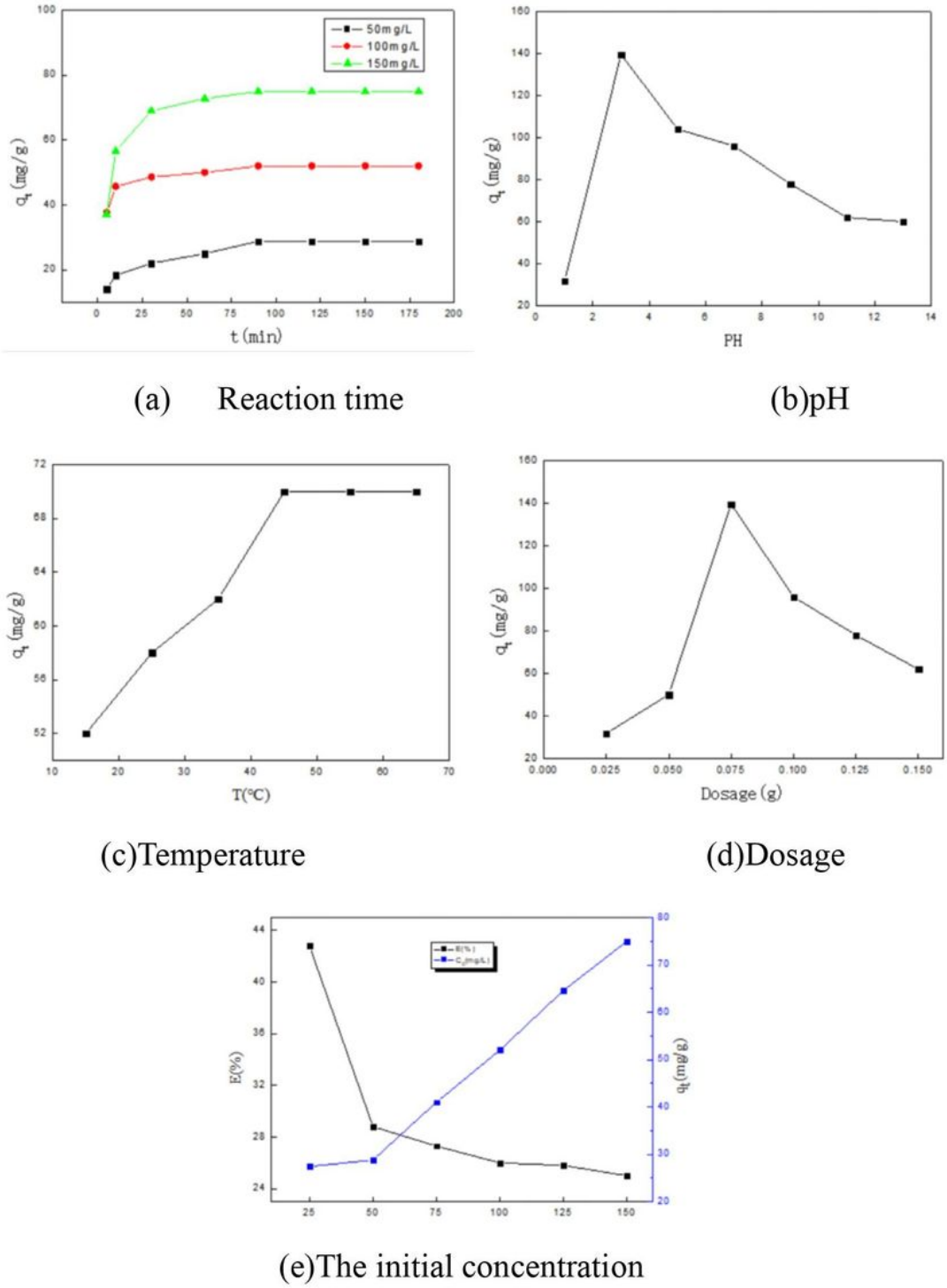

Figure 1

Varying factor effects on Cr (VI) removal in aqueous solution: (a) pH value; (b) dosage; (c) reaction time as well as (d) original Cr (VI) content.

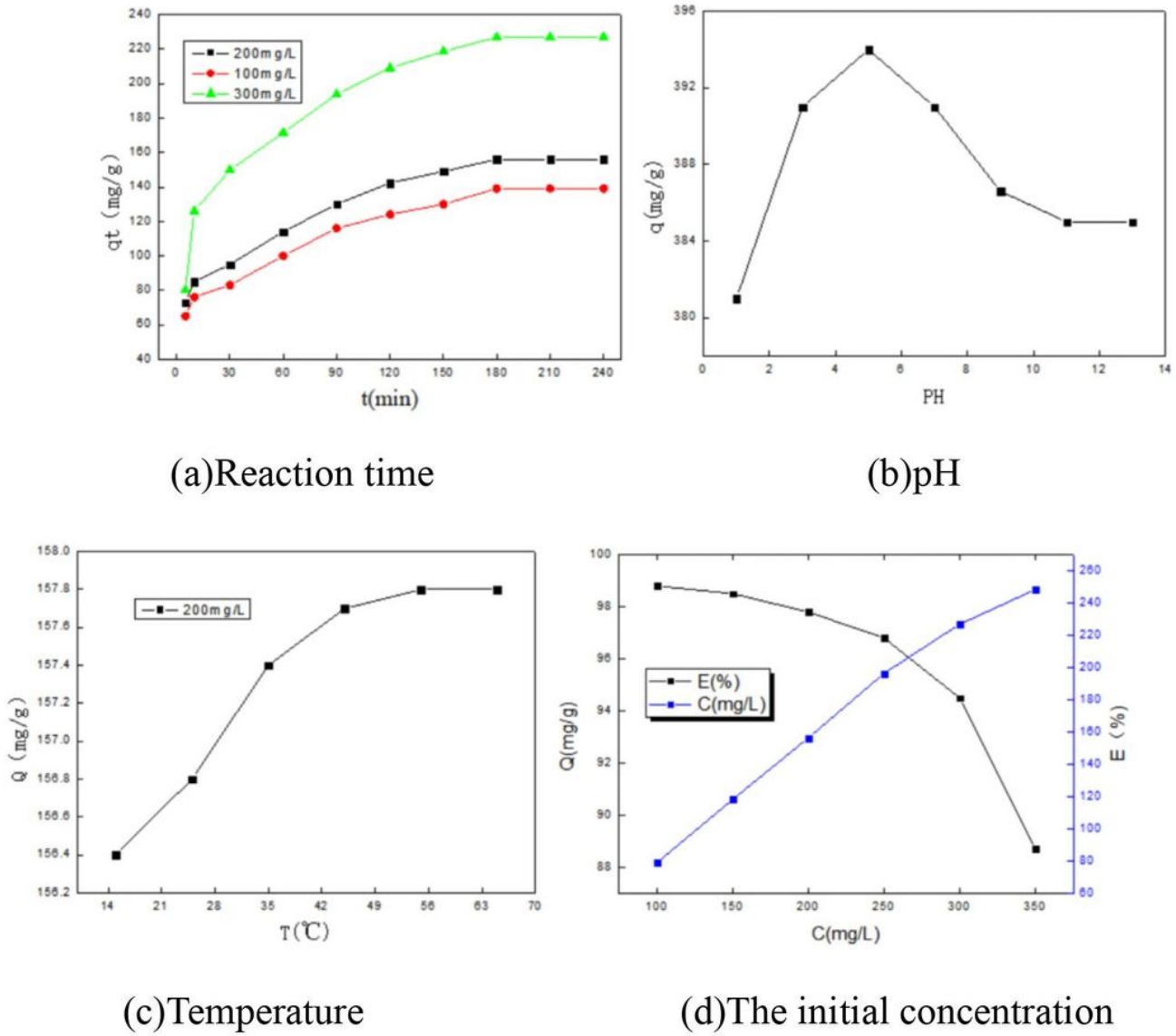

Figure 2

Varying factor effects on Cu (II) removal in aqueous solution: (a) pH value; (b) dosage; (c) reaction time as well as (d) original Cu (II) content.

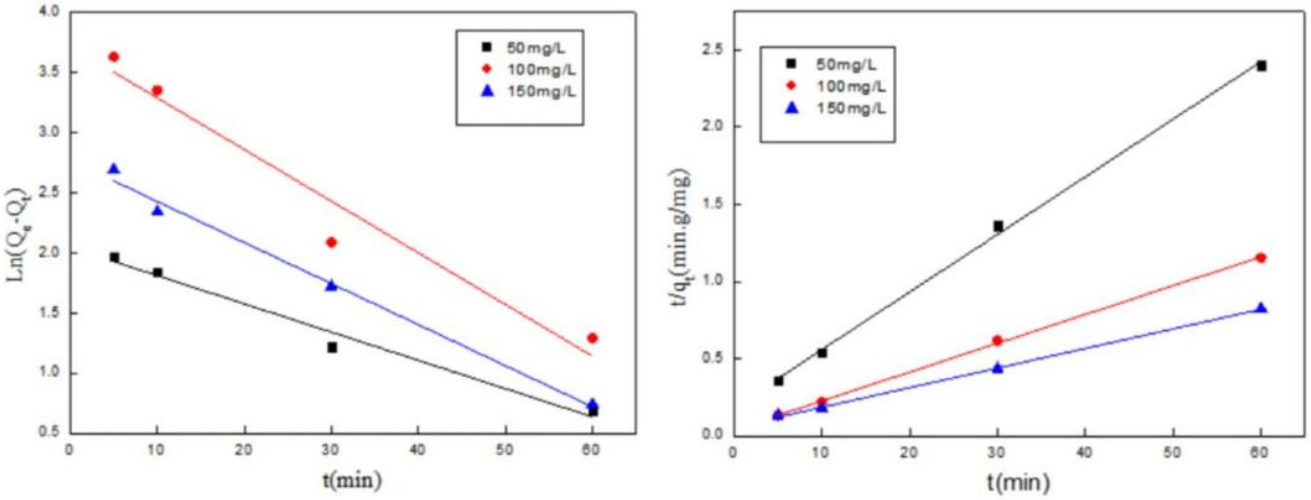

Figure 3

Quasi-first-order and quasi-second-order kinetic equations on adsorption of Cr(VI)

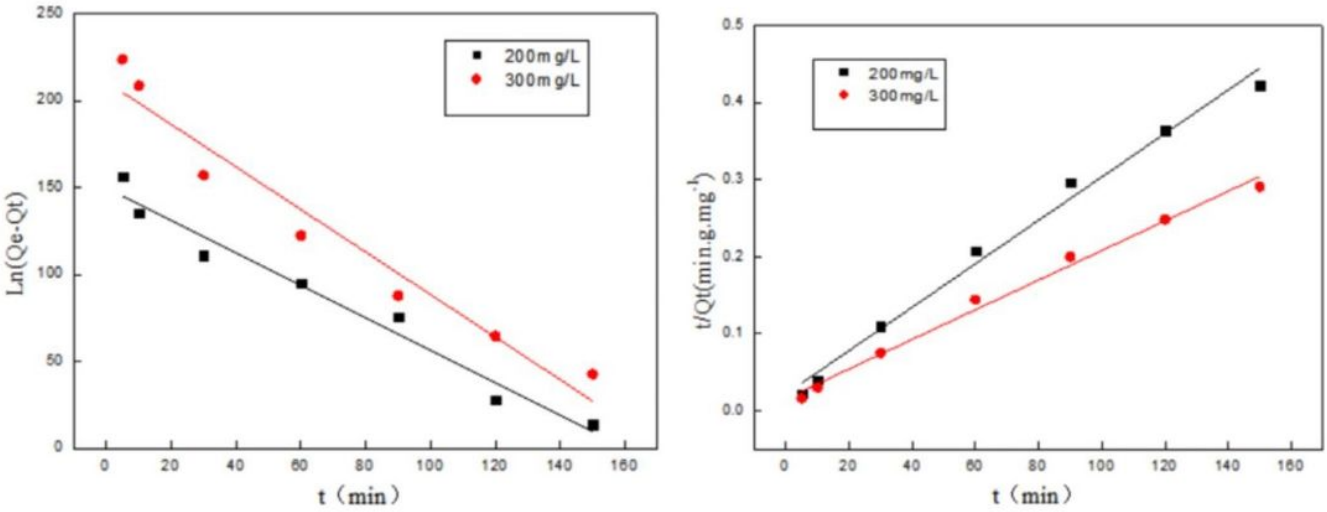

Figure 4

Quasi-first-order and quasi-second-order kinetic equations on adsorption of Cu(II)

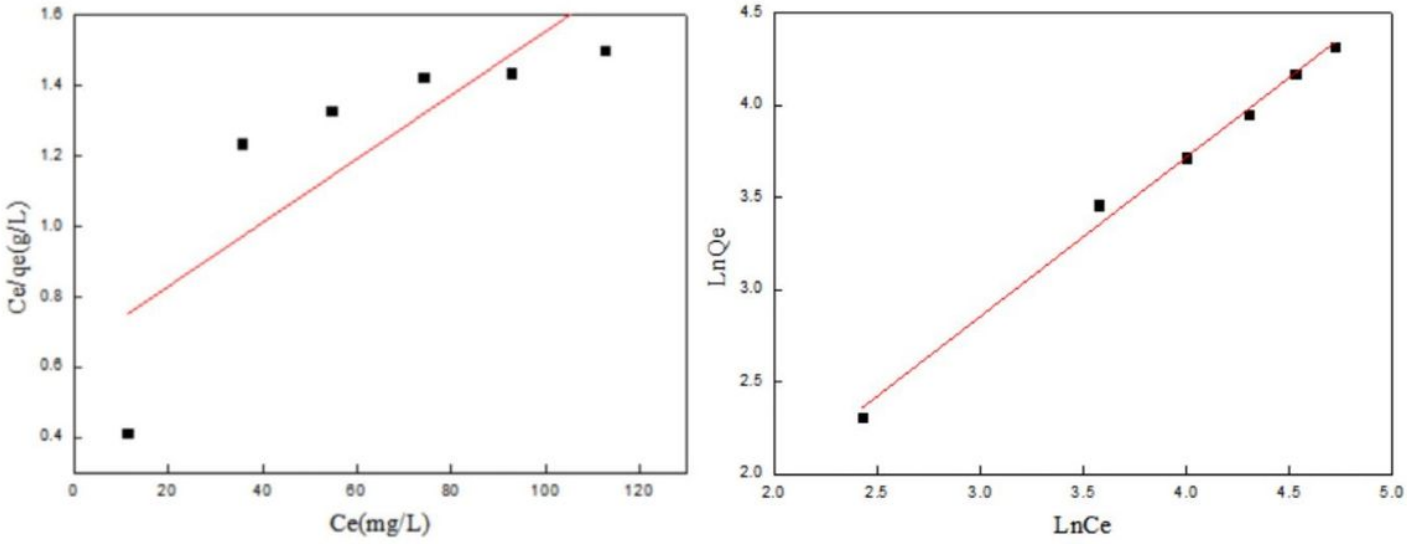

Figure 5

Adsorption isotherm of Cr(VI)

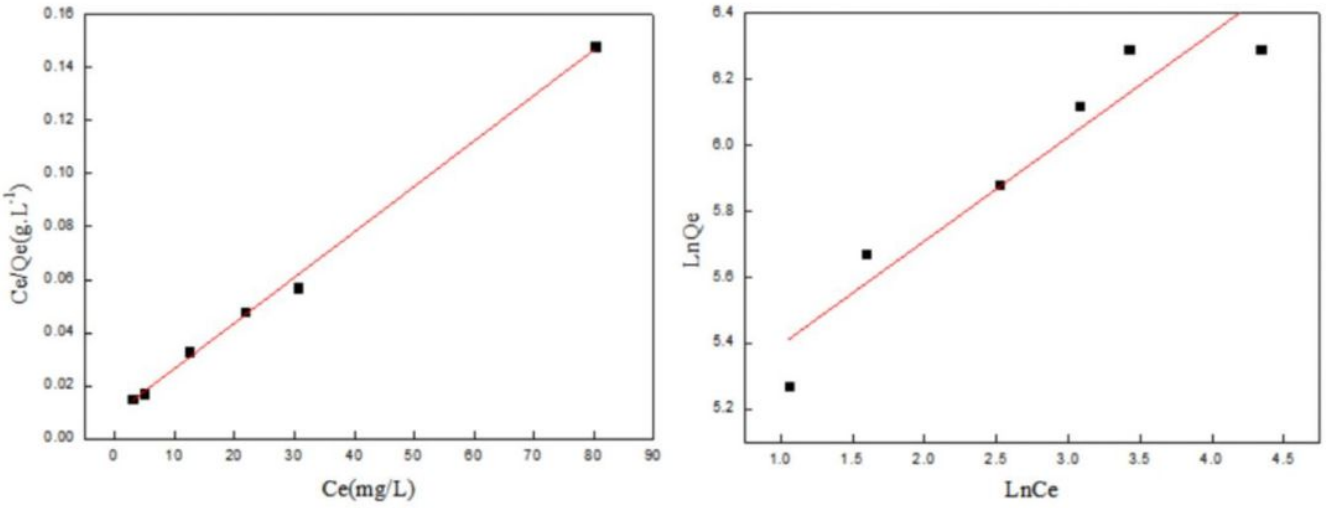

Figure 6

Adsorption isotherm of Cu(II)

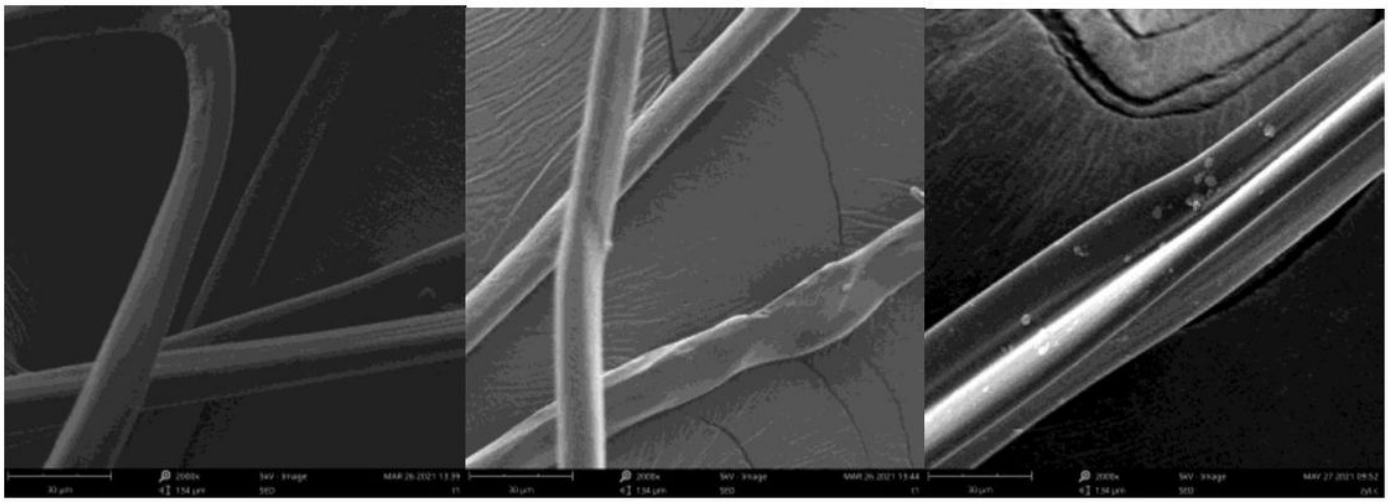

(a) (b) (c)

Figure 7

CS SEM images before and (b) after the reactionwith Cr(VI)and(c) with Cu(II).

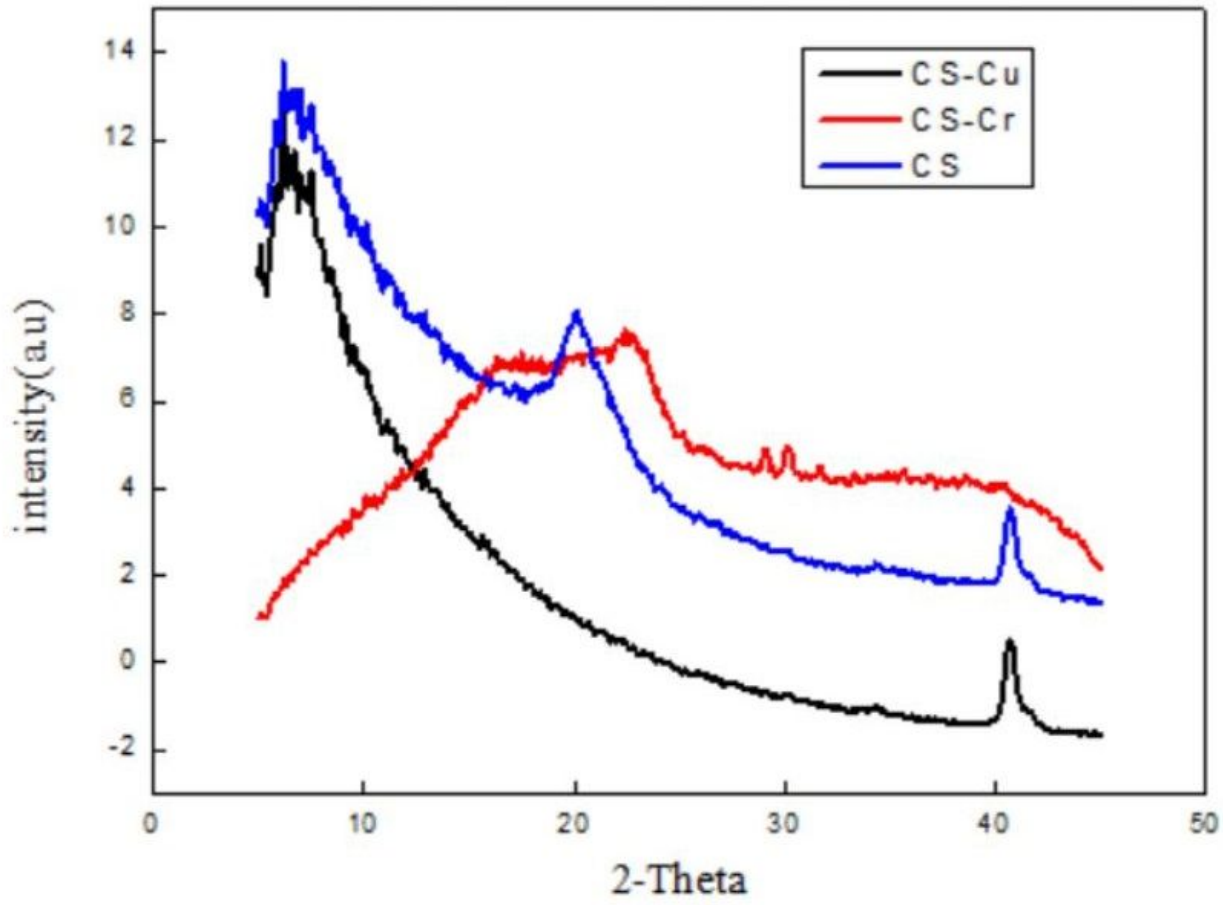

Figure 8

XRD of CS before and after use for Cr (VI) and Cu(II) adsorption.

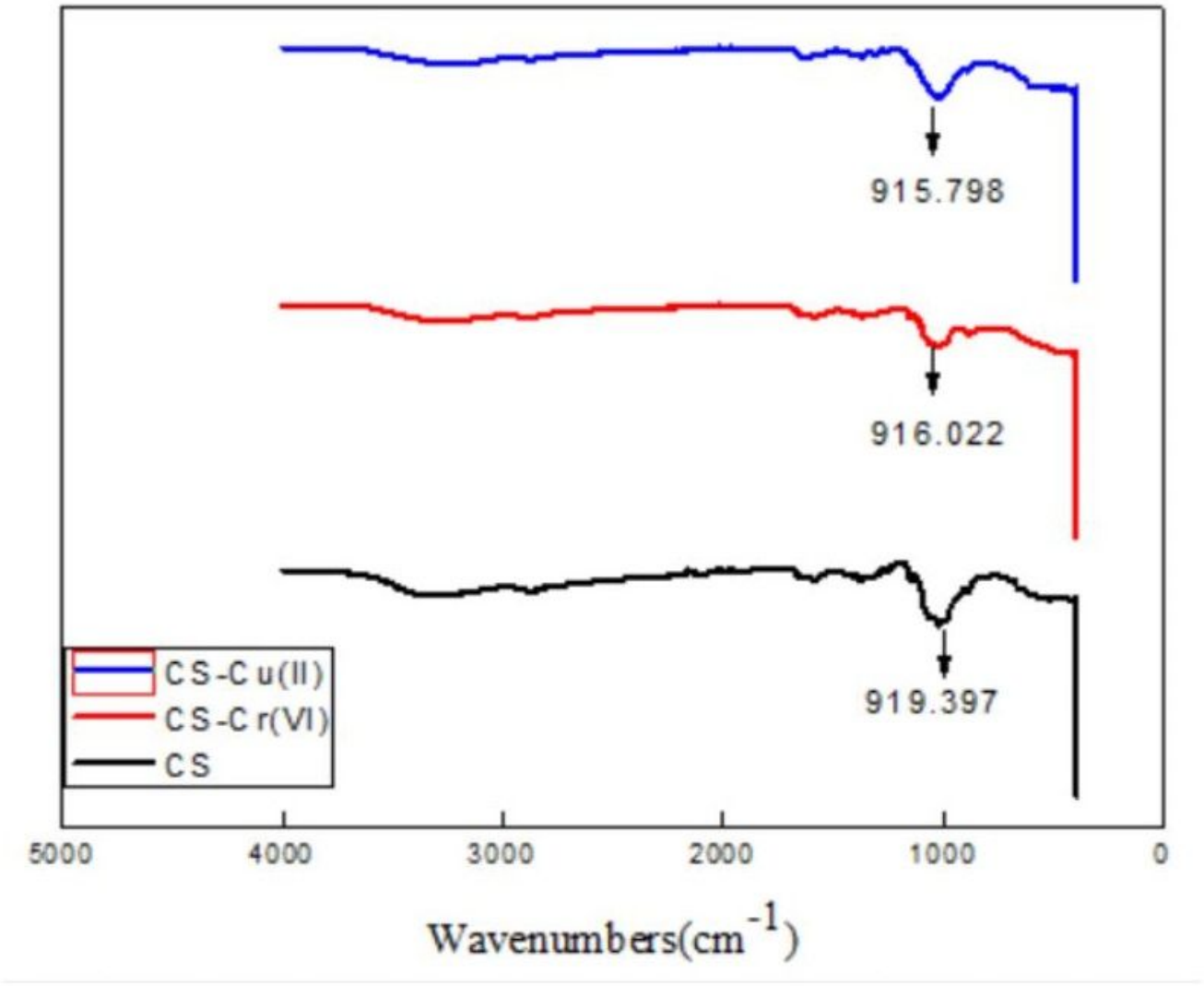

Figure 9

FTIR of CS before and after use for Cr (VI) and Cu(II) adsorption.